JACS
JOURNAL OF THE AMERICAN CHEMICAL SOCIETY

Article

pubs.acs.org/JACS

Suppression of Lithium Dendrite Growth Using Cross-Linked Polyethylene/Poly(ethylene oxide) Electrolytes: A New Approach for Practical Lithium-Metal Polymer Batteries

Rachna Khurana,[†] Jennifer L. Schaefer,[‡] Lynden A. Archer,*[,‡] and Geoffrey W. Coates*[,†]

[†]Department of Chemistry and Chemical Biology, Baker Laboratory, Cornell University, Ithaca, New York 14853, United States
[‡]School of Chemical and Biomolecular Engineering, Olin Hall, Cornell University, Ithaca, New York 14853, United States

Supporting Information

ABSTRACT: Solid polymer electrolyte (SPE) membranes are a critical component of high specific energy rechargeable Li-metal polymer (LMP) batteries. SPEs exhibit low volatility and thus increase the safety of Li-based batteries compared to current state-of-the-art Li-ion batteries that use flammable small-molecule electrolytes. However, most SPEs exhibit low ionic conductivity at room temperature, and often allow the growth of lithium dendrites that short-circuit the batteries. Both of these deficiencies are significant barriers to the commercialization of LMP batteries. Herein we report a cross-linked polyethylene/poly(ethylene oxide) SPE with both high ionic conductivity (>1.0 × 10^{-4} S/cm at 25 °C) and excellent resistance to dendrite growth. It has been proposed that SPEs with shear moduli of the same order of magnitude as lithium could be used to suppress dendrite growth, leading to increased lifetime and safety for LMP batteries. In contrast to the theoretical predictions, the low-modulus (G' ≈ 1.0 × 10^5 Pa at 90 °C) cross-linked SPEs reported herein exhibit remarkable dendrite growth resistance. These results suggest that a high-modulus SPE is not a requirement for the control of dendrite proliferation.

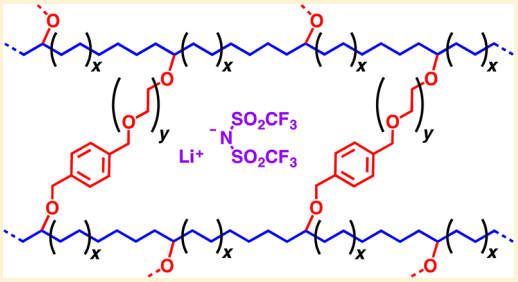

INTRODUCTION

Current rechargeable Li-ion batteries (LIBs) are important constituents of portable electronics, stationary grid-energy storage components, and hybrid/electric vehicles.[1−3] LIB technologies have enabled the transformation of the consumer electronics market since their launch in 1991 by the Sony Corporation; however these LIBs contain flammable organic liquids as an electrolyte component that raises safety concerns.[4] Several incidents including the recent fires in the LIB unit of Tesla Model S and a Boeing 787 Dreamliner airplane have raised questions about the safety of using LIBs for transportation applications.[5] Furthermore, the specific energy density of current state-of-the-art LIBs is below the U.S. Department of Energy Vehicle Technologies Program's long-term target for the secondary batteries.[6] The low energy density of these batteries has been one of the roadblocks for the ultimate replacement of internal combustion vehicles by electric vehicles. Replacing flammable electrolytes and enhancing the energy density of Li-based battery technologies are at the forefront of research in both academia and industry.[3,7,8]

A rechargeable Li-metal-based battery is considered to be one of the most promising technologies for energy storage devices due to its high theoretical storage capacity, which is facilitated by the use of lithium (Li) metal, instead of lithiated graphite (3800 mA h g^{-1} compared to 380 mA h g^{-1}, respectively).[9] Despite these attractive features, the use of Li metal in conjunction with liquid electrolytes is currently limited by the formation of irregular Li electrodeposits (dendrites) during repeated charge−discharge cycles.[10] These dendrites can ultimately span the interelectrode space, short circuit the cell and cause overheating and thermal runaway. Many approaches have been proposed in the literature to delay dendrite nucleation, including alloying Li anodes with other metals[11,12] and using additives to improve the uniformity at the solid−electrolyte interface (SEI).[13−16] Although these strategies are promising, the performance suffers due to a reduced anode capacity, and durability is lowered by consumption of additives during the formation of the SEI films over successive charge−discharge cycles. An important scientific goal is the development of a solid polymer electrolyte (SPE) that inhibits dendrite growth. There are two main theoretical frameworks for understanding dendrite nucleation and propagation in an electrolyte. The Chazalviel model proposes that dendrites arise from dissimilar transport of cations and anions in an electrolyte. Specifically, anion depletion is predicted to produce large electric fields near the lithium electrode that leads to enhanced electrodeposition on the Li-metal surface causing dendrites to grow. Electrolytes with higher ionic conductivity and reduced anion mobility will delay dendrite nucleation by mitigating anion depletion near the electrode−electrolyte interface.[17] Rosso and co-workers demonstrated agreement between the

Received: March 1, 2014
Published: April 22, 2014

   dx.doi.org/10.1021/ja502133j | J. Am. Chem. Soc. 2014, 136, 7395−7402

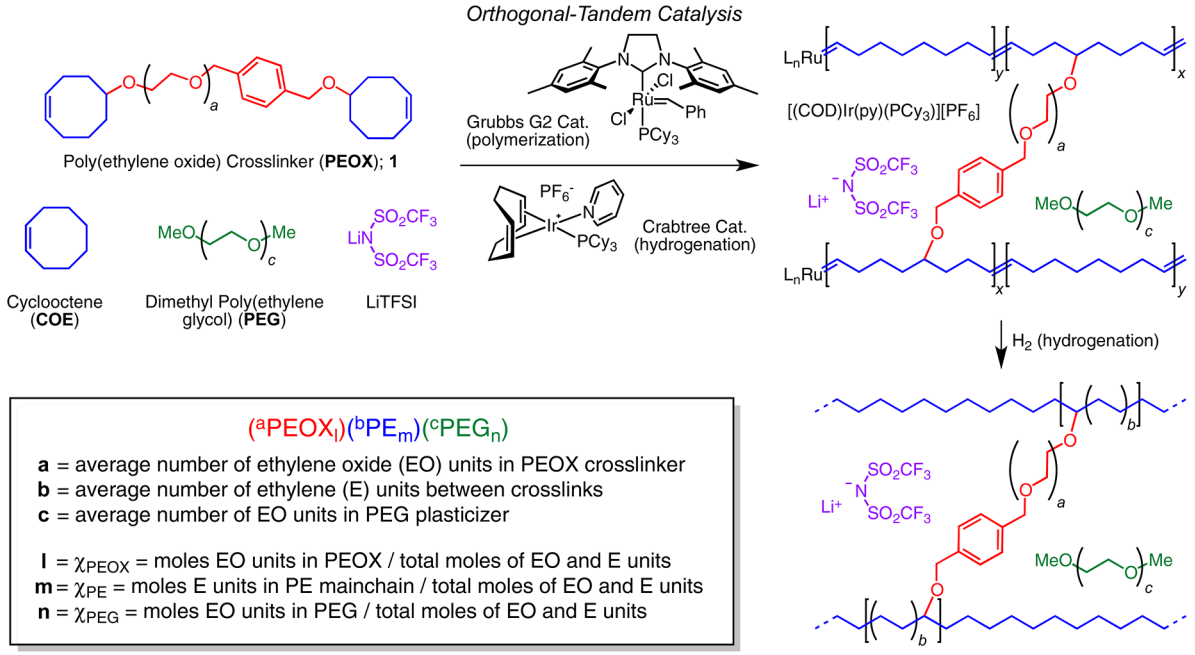

Figure 1. Polyethylene/poly(ethylene oxide) solid polymer electrolyte (SPE) synthesis and nomenclature.

Chazalviel model and measured short-circuit lifetimes of lithium metal cells employing poly(ethylene oxide) (PEO) electrolytes.[18] In addition, a second framework due to Newman and Monroe considers the effect of physical variables such as electrolyte/separator modulus and surface tension on the kinetics of lithium electrodeposition. A prediction from this model is that SPEs with high shear modulus ($G' > 7$ GPa) could be used to suppress the dendrite growth.[19] Balsara and co-workers cleverly designed mechanically rigid ($G' \approx 0.1$ GPa) microphase-separated polystyrene-*b*-poly(ethylene oxide) (PS-*b*-PEO) block copolymers that showed high resistance to Li dendrite growth, supporting the high modulus theory.[20] Due to the semicrystallinity of the PEO phase, the PS-*b*-PEO block polymers only exhibited high ionic conductivities ($>1.0 \times 10^{-4}$ S/cm) above 90 °C.[21] Inspired by this important advance in dendrite resistance, we anticipated there might be SPE architectures that simultaneously exhibit higher ionic conductivities at room temperature without sacrificing resistance to Li dendrite growth.

Electrolyte membranes incorporating PEO with a lithium salt have long been proposed as viable candidates for LMP batteries.[22,23] However, such SPEs have poor conductivities at room temperature due to the crystallinity of PEO. Cross-linking is one of the many ways to suppress the crystallization of PEO; it increases the amount of amorphous phase in the polymer and gives the polymer rubber-like characteristics.[24,25] To date, numerous PEO-based cross-linked polymers have been investigated for lithium-battery applications including polyether copolymers,[26−30] acrylate polymers,[31,32] and polyurethane network polymers.[33] Although these network polymers are mechanically rigid, low ionic conductivities at room temperature ($\sim 1.0 \times 10^{-5}$ S/cm) limit their application. To increase the conductivity of network polymers, researchers have studied various plasticized SPEs that contain additives such as ionic liquids[34−37] and low-molecular weight methoxy-terminated poly(ethylene glycol).[38−41] While all of these systems improve LMP battery performance, none of them meets all the required standards, i.e. lasting resistance to dendrite growth and high ionic conductivity of the freestanding polymer film at ambient temperature. Moreover, none of these PEO-based cross-linked SPEs have been tested quantitatively to demonstrate their ability to prevent lithium dendrite growth on the anode. To the best of our knowledge, there are only two reports of poly(methyl methacrylate)[42] and poly(acrylonitrile)[43] based cross-linked gel polymer electrolytes that have been shown, using qualitative optical microscopy experiments, to inhibit dendrite growth; however, even these systems had to be plasticized with volatile nonaqueous electrolyte components, which partially defeats the purpose of using an SPE to enhance cell safety.

Herein, we report our work on a new family of Li-ion conducting SPEs composed of stiff semicrystalline polyethylene (PE) chains covalently cross-linked by PEO segments. Our synthetic route to these unique SPE structures offers the advantage of tuning the PE backbone length between cross-links as well as the PEO segment lengths, which provides precise suppression of PEO crystallinity that affects ionic conductivity. Most importantly, these polymer electrolytes display both high ionic conductivity and superior dendrite growth suppression.

RESULTS AND DISCUSSION

We recently reported the synthesis of high-performance cross-linked alkaline anion-exchange membranes for fuel cell applications using a ring-opening metathesis polymerization (ROMP) route.[44] We expected that a similar synthetic strategy could be used to create a PEO-based Li-ion conducting polymer electrolyte that could also act as an effective separator in the lithium battery. We designed an SPE that is cross-linked with PEO segments and contains a polyethylene (PE) backbone using an orthogonal-tandem catalysis approach[45] (Figure 1). Constraining the PEO chains by incorporating them into a cross-linker reduces the crystallinity of PEO in the copolymers. Poly(ethylene oxide) cross-linker, **PEOX** (**1**) was readily synthesized from inexpensive starting materials in excellent yields.[46] Cyclooctene (**COE**) was copolymerized

dx.doi.org/10.1021/ja502133j | J. Am. Chem. Soc. 2014, 136, 7395−7402

Table 1. Compositions and DC Ionic Conductivities of Unplasticized PE-PEO Cross-Linked SPEs[a]

			PE segments[b]		PEO segments[c]				
entry	unplasticized SPE	[COE]:[1] ratio	T_m[d] (°C)	ΔH_{fus}[d] (J/g)	T_g[d] (°C)	T_c[d] (°C)	T_m[d] (°C)	ΔH_{fus}[d] (J/g)	DC Ionic conductivity at 25 °C[e] (S/cm)
1	$(^{33}PEOX_{0.32})(^{34}PE_{0.68})$	15:1	89	20.0	−45	n.d.[f]	n.d.[f]	n.d.[f]	5.2×10^{-6}
2	$(^{33}PEOX_{0.40})(^{24}PE_{0.60})$	10:1	82	14.8	−45	n.d.[f]	n.d.[f]	n.d.[f]	9.0×10^{-6}
3	$(^{33}PEOX_{0.47})(^{18}PE_{0.53})$	7:1	61	6.4	−43	n.d.[f]	n.d.[f]	n.d.[f]	8.3×10^{-6}
4	$(^{76}PEOX_{0.51})(^{34}PE_{0.49})$	15:1	94	11.8	−49	−20	23	5.4	2.3×10^{-5}
5	$(^{76}PEOX_{0.60})(^{24}PE_{0.40})$	10:1	88	10.1	−50	−19	26	9.4	2.8×10^{-5}
6	$(^{76}PEOX_{0.66})(^{18}PE_{0.34})$	7:1	74	2.9	−48	−14	25	5.6	3.1×10^{-5}
7	$(^{123}PEOX_{0.64})(^{34}PE_{0.36})$	15:1	111	10.1	−38	n.d.[f]	39	18.6	8.2×10^{-6}
8	$(^{123}PEOX_{0.72})(^{24}PE_{0.28})$	10:1	103	1.2	−39	n.d.[f]	37	12.6	8.4×10^{-6}
9	$(^{123}PEOX_{0.77})(^{18}PE_{0.23})$	7:1	97	1.1	−38	n.d.[f]	38	16.1	7.4×10^{-6}

[a]All films had [EO]:[Li] composition of 18:1; where EO means ethylene oxide units in the PEOX cross-linker. [b]PE segments: polyethylene domains in the polymer electrolyte. [c]PEO segments: poly(ethylene oxide) domains in the polymer electrolyte. [d]Glass transition temperature (T_g), cold crystallization temperature (T_c), and melting temperature (T_m) were determined by differential scanning calorimetry of the second heat cycle. [e]Determined by dielectric spectroscopy measurements. See Supporting Information (SI) for more details. [f]Not detected.

with **1** in the presence of Grubbs' second-generation catalyst (G2 catalyst) in THF in a fluoropolymer-lined dish.[47] After slow evaporation of the solvent at 50 °C, thin translucent films were obtained. Upon hydrogenation of these unsaturated films catalyzed by the iridium catalyst trapped within the amorphous cross-linked matrix,[48] the mechanical strength of membranes greatly improved, and they were further examined by electrochemical tests. Some of the SPEs were designed to include controlled fractions of free methoxy-terminated poly(ethylene glycol) (**PEG**) oligomers as plasticizers to assess their effect on conductivity and mechanical properties of the membranes. To gain better understanding of this PE-PEO cross-linked solid polymer electrolyte system, a variety of polymer electrolyte samples were prepared by varying the cross-linker length, [**COE**]:[**1**] ratio, and weight percentage (wt %) of the plasticizer. To evaluate the effect of cross-linker length on the ionic conductivity of the SPEs, three **PEOX** cross-linkers with 33, 76, and 123 ethylene oxide (EO) repeat units were synthesized.[49] Nine different SPEs were prepared using three different cross-linkers and at three different [**COE**]:[**1**] ratios (Table 1). The nomenclature used for these SPEs is described in Figure 1; each component in the SPE is given a symbol (e.g., **PEOX** for the PEO cross-linker), the numbers of repeat units for each of the components are shown in the superscripts, and the mole fraction of the units in the SPE is given in the subscripts.

The compositions and thermal properties of all the cross-linked PE-PEO-based SPEs are listed in Table 1. The SPEs containing the cross-linker with 33 EO units (^{33}PEOX: entries 1−3), showed no melting transition (T_m) of the PEO segments, indicating that the PEO domains of the cross-linked SPE are essentially amorphous. Interestingly, electrolytes with 76 EO units in the cross-linker (^{76}PEOX: entries 4−6), exhibited glass transition temperatures (T_gs) of about −49 °C which are lower than the T_gs observed for ^{33}PEOX SPEs ($T_g \approx -44$ °C), suggesting moderately enhanced segmental motion of the PEO in ^{76}PEOX electrolytes. Furthermore, ^{76}PEOX SPEs exhibited both cold crystallization temperatures (T_cs) and T_ms near room temperature in the PEO segments during the heating cycle of the DSC, while no crystallization temperature was observed in the cooling cycle on DSC. This can be attributed to the low cross-linking density of the network polymers, allowing the PEO chains to rearrange and crystallize in the network when enough energy is provided in the heating cycle during DSC.[50]

For the SPEs containing 123 EO units (^{123}PEOX: entries 7−9), T_ms of around 38 °C were observed and the T_gs were much higher than those of polymer electrolytes containing 33 and 76 EO units in the cross-linker, suggesting that the PEO functionalized cross-linker length was too large to prevent the crystallization of PEO in the network structure. Furthermore, among the polymer electrolytes with different cross-linker lengths and the same ratio of [**COE**]:[**1**] (e.g., comparison of entries 1, 4, and 7), ^{33}PEOX polymer electrolytes had the smallest PE crystallites in the network (lowest T_m), which could be explained by the relatively higher cross-linking density in these SPEs that inhibited the PE crystallization in the network. Also, for polymer electrolytes having the same cross-linker length (e.g., entries 1−3), higher [**COE**]:[**1**] ratios yielded materials with better mechanical integrity.

The ionic conductivities of the unplasticized SPEs were tested, and the values are reported in Table 1. It is clear that there is a significant effect of **PEOX** length on the ionic conductivity of the polymer electrolytes (e.g., comparison of ionic conductivities of entries 1, 4, and 7 at constant [**COE**]:[**1**] ratio). However, no substantial changes in ionic conductivities were observed when the number of ethylene repeat units between the cross-links was changed by varying the [**COE**]:[**1**] ratio (e.g., comparison of ionic conductivities of ^{76}PEOX electrolytes: entries 4, 5, and 6). Although PEO domains in the ^{33}PEOX SPEs were completely amorphous (no T_m) and ^{76}PEOX electrolytes had crystalline PEO domains in the network structure, ^{76}PEOX electrolytes exhibited the highest ionic conductivities (averaging 2.7×10^{-5} S/cm), which are roughly 3 times more than that observed for the ^{33}PEOX and ^{123}PEOX electrolytes ($<10^{-5}$ S/cm) and more than 4 times higher than the PEO-LiTFSI (σ of 7.2×10^{-6} S/cm at [EO]:[Li] 18:1 and 25 °C). We postulate that the surprisingly high ionic conductivity of the ^{76}PEOX electrolytes is a direct consequence of the low T_g of these SPEs, allowing enhanced segmental motion of PEO in the amorphous domains thus facilitating lithium-ion conduction. Among the ^{76}PEOX electrolytes tested, $(^{76}PEOX_{0.66})(^{18}PE_{0.34})$ exhibited maximum ionic conductivity (3.1×10^{-5} S/cm at 25 °C), which is comparable to those reported by other research groups for amorphous PEO network polymers. For instance, Watanabe and co-workers reported the conductivity value of 2×10^{-5} S/cm at 20 °C for a network poly(ethylene oxide)-*co*-poly(propylene oxide) copolymer with LiTFSI salt.[26] Armand and co-workers observed

dx.doi.org/10.1021/ja502133j | J. Am. Chem. Soc. 2014, 136, 7395−7402

Table 2. Compositions of Plasticized PE-PEO Cross-Linked SPEs[a]

			PE segments[c]		PEO segments[d]			
entry	plasticized SPE	weight % plasticizer (^{5}PEG)[b]	T_m[e] (°C)	ΔH_{fus}[e] (J/g)	T_g[e] (°C)	T_c[e] (°C)	T_m[e] (°C)	ΔH_{fus}[e] (J/g)
1[f]	(^{70}PEOX$_{0.50}$)(^{34}PE$_{0.50}$)	0	91	15.2	−47	−14	20	10.1
2[f]	(^{70}PEOX$_{0.43}$)(^{34}PE$_{0.43}$)(^{5}PEG$_{0.14}$)	16	91	14.8	−54	−22	15	8.3
3[f]	(^{70}PEOX$_{0.39}$)(^{34}PE$_{0.39}$)(^{5}PEG$_{0.22}$)	24	97	19.5	−57	−22	16	12.8
4[f]	(^{70}PEOX$_{0.34}$)(^{34}PE$_{0.35}$)(^{5}PEG$_{0.31}$)	31	95	20.1	−61	−26	18	14.9
5[f]	(^{70}PEOX$_{0.30}$)(^{34}PE$_{0.31}$)(^{5}PEG$_{0.39}$)	39	96	14.8	−65	−29	14	11.6
6[g]	(^{5}PEG$_{1.00}$)	75	n.a.[h]	n.a.[h]	−88	n.d.[i]	n.d.[i]	n.d.[i]

[a]All films had [EO]:[Li] composition of 18:1; where EO includes ethylene oxide units contained both in the PEOX cross-linker and PEG plasticizer. [b]Wt % of **PEG** plasticizer = [(mass of **PEG**)/{(mass of **PEG**) + (mass of **PEOX**) + (mass of **COE**) + (mass of **LiTFSI**)}] × 100. [c]PE segments: Polyethylene domains in the polymer electrolyte. [d]PEO segments: Poly(ethylene oxide) domains in the polymer electrolyte. [e]Glass transition temperature (T_g), cold crystallization temperature (T_c), and melting temperature (T_m) were determined by differential scanning calorimetry of the second heat cycle. [f]All films had 70 EO units in the cross-linker and [**COE**]:[**1**] loading of 15:1. [g]Sample ^{5}PEG$_{1.00}$:dimethyl poly(ethylene glycol), M_n 275 Da with [EO]:[Li] composition of 18:1 for comparison purposes. [h]Not applicable. [i]Not detected.

conductivity of 1 × 10^{-5} S/cm at 25 °C for their PEO-based network polymer electrolytes.[28] Even though the ionic conductivity values of these PE-PEO cross-linked SPEs are similar to the other PEO-based unplasticized network polymers reported in the literature, we hypothesized that our unique polymer electrolyte design could prove advantageous for an LMP separator, because these network SPEs have mechanically strong and electrochemically stable polyethylene segments, which chemically resemble commercially available separators.[51]

It has been proposed that ionic conductivities greater than 1 × 10^{-4} S/cm are necessary for SPEs to function in commercial batteries that require ambient temperature operation.[1] However, PEO polymers exhibit low conductivity (<1 × 10^{-4} S/cm) at room temperature due to the crystalline domains.[52] Recently, Hawker and co-workers reported a copolymer of ethylene oxide and allyl glycidyl ether that showed an ionic conductivity of 5 × 10^{-5} S/cm at 25 °C.[53] We were able to achieve similar ionic conductivities for some PEO-based cross-linked SPEs (Table 1, entries 4−6), while still retaining good mechanical properties. Once the unplasticized SPE with the highest ionic conductivity was identified (2.7 × 10^{-5} S/cm at 25 °C for ^{76}PEOX SPEs), poly(ethylene glycol) dimethyl ether (**PEG**; M_n 275 Da and flash point 156 °C) was added as a plasticizer to improve the ionic conductivity and support higher charge/discharge rates. Since the (^{76}PEOX$_{0.51}$)(^{34}PE$_{0.49}$) sample exhibited better mechanical integrity, samples of this composition were prepared with varying amounts of **PEG** (16, 24, 31, and 39 wt %) to obtain plasticized cross-linked SPEs.[54] Compositions and thermal characteristics of the plasticized samples are reported in Table 2. Addition of plasticizer led to a significant decrease in T_g from −47 °C (0 wt % **PEG**) to −65 °C (39 wt % **PEG**). Also, a significant decrease in the T_c and T_m corresponding to the PEO segments in the plasticized SPEs (entries 1−5) was observed, indicating that the PEO crystallization is hindered by incorporating small PEG oligomers into the cross-linked network. The temperature-dependent ionic conductivities of these cross-linked plasticized SPEs at various wt % of **PEG** (16, 24, 31, 39 wt %) are shown in Figure 2. Notably, the SPE with 39 wt % **PEG** (entry 5) showed an ionic conductivity value of 2.0 × 10^{-4} S/cm, which is an order of magnitude higher than the unplasticized SPE (0 wt % plasticizer; entry 1). By comparison, Mastragostino and coauthors developed a **PEG** (M_n 500 Da)-doped PEO-based polyurethane network polymer that showed a conductivity of 1.0 × 10^{-5} S/cm at 25 °C; however they did not observe a significant increase in conductivity upon addition of plasticizer.[40] Park and co-workers reported an interesting plasticized SPE, wherein they incorporated **PEG** (M_n 250 Da) and PEO-based cross-linked electrolyte inside the pores of a PE nonwoven matrix. The resulting SPE with 20 wt % cross-linking agent and 80 wt % nonvolatile plasticizer displayed conductivity of 3.1 × 10^{-4} S/cm at room temperature.[55] Kang and co-workers recently reported a multiarmed plasticizer-doped PEO/siloxane-based cross-linked polymer, which exhibited a conductivity value of 1.0 × 10^{-4} S/cm at 25 °C.[38] While all of these plasticized SPEs reported in the literature offer major improvements in conductivity for solid polymer electrolytes, none has been tested for its ability to influence lithium dendrite nucleation and growth in a battery.

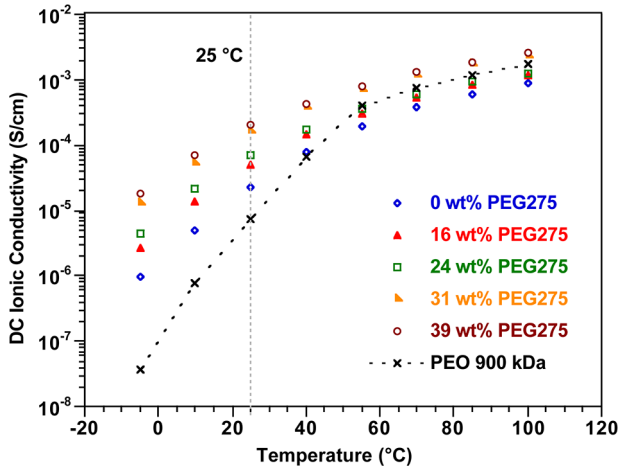

Figure 2. Plot of DC ionic conductivity as a function of temperature for ^{70}PEOX electrolytes having different weight percent of PEG275 plasticizer. All films had [COE]:[**1**] ratio of 15:1 and [EO]:[Li] composition of 18:1. The conductivity of a PEO 900 kDa sample with [EO]:[Li] ratio of 18:1 is also shown for comparison purposes.

Inspired by the dendrite studies reported by Balsara and co-workers,[20] we performed galvanostatic lithium plate/strip electrochemical cycling measurements in symmetric Li/SPE/Li cells to quantify the effect of our PE-PEO cross-linked SPEs on the lifetime of lithium-metal-based batteries. Measurements were performed at variable current densities, J, using a 3 h lithium plating followed by a 3 h lithium stripping routine designed to ensure that, in the event of unstable electrodeposition, sufficient quantities of lithium is transported during each cycle to produce dendrites that bridge the interelectrode space and short-circuit the cell. The SPE's resistance to

dx.doi.org/10.1021/ja502133j | J. Am. Chem. Soc. 2014, 136, 7395−7402

dendrite growth is here quantified in terms of total charge passed, C_d, at the time of cell failure by dendrite-induced short-circuits.[49] At a current density of 0.5 mA/cm^2 and measurement temperature of 90 °C the unplasticized solid polymer electrolyte, (^{70}PEOX$_{0.50}$)(^{34}PE$_{0.50}$) with only a modest shear modulus ($G' \approx 10^5$ Pa at 90 °C), displays an order of magnitude higher C_d value (1185 C/cm^2 at J = 0.50 mA/cm^2 and 90 °C) than reported for high modulus PS-*b*-PEO block copolymers (105 C/cm^2 at J = 0.26 mA/cm^2 and 90 °C).[20] Our finding demonstrates that a separator exhibiting high shear storage modulus is not a requirement to inhibit dendrite growth. Since it took about a month to short-circuit this cell operating near the upper threshold of current density allowed by the unplasticized SPE, we selected one sample, (^{70}PEOX$_{0.34}$)(^{34}PE$_{0.35}$)(^{5}PEG$_{0.31}$), a plasticized SPE (31 wt % **PEG**) with high ionic conductivity ($\sigma \approx 1.6 \times 10^{-4}$ S/cm at 25 °C) and reasonable storage modulus ($G' \approx 1.0 \times 10^5$ Pa at 90 °C), to measure C_d at variable current densities (0.26 mA/cm^2–1.3 mA/cm^2) and 90 °C.

Figure 3a reports C_d values as a function of current density for a high molar mass PEO standard (M_n 900 kDa) and (^{70}PEOX$_{0.34}$)(^{34}PE$_{0.35}$)(^{5}PEG$_{0.31}$). The PE-PEO cross-linked SPE displayed significantly higher C_d values than observed for PEO (M_n 900 kDa) sample at all the measured current density values. Notably, it displayed a C_d value of 1790 C/cm^2 that is more than an order of magnitude greater than that reported for PS-*b*-PEO block copolymers (C_d value of 105 C/cm^2) under the same testing conditions (0.26 mA/cm^2 and 90 °C).[56] At higher current density values (>0.26 mA/cm^2), the cells short-circuit faster, and C_d values are consequently lower. Significantly, even under these harsher measurement conditions (cells cycled at significantly higher current density), the PE-PEO cross-linked SPE displayed a higher C_d value (156 C/cm^2 at J = 1.30 mA/cm^2 and 90 °C) compared to PS-*b*-PEO block copolymer (105 C/cm^2 at J = 0.26 mA/cm^2 and 90 °C). Recently, Balsara and co-workers reported TiO_2-doped PS-*b*-PEO block copolymer, that showed better dendrite growth suppression than the PS-*b*-PEO block copolymers (C_d value of 1766 C/cm^2 compared to 374 C/cm^2 at 0.17 mA/cm^2 and 90 °C).[57,58] The SPE reported herein, i.e. (^{70}PEOX$_{0.34}$)(^{34}PE$_{0.35}$)(^{5}PEG$_{0.31}$), displayed a C_d value (1790 C/cm^2 at 0.26 mA/cm^2 and 90 °C; 3 h charge–discharge cycle) comparable to those exhibited by TiO_2-doped PS-*b*-PEO block copolymer (1766 C/cm^2 at 0.17 mA/cm^2 and 90 °C; 4 h charge–discharge cycle). This result is notable because the dendrite tests for PE-PEO cross-linked copolymer were conducted at higher current density compared to that for TiO_2-doped PS-*b*-PEO block copolymer (0.26 mA/cm^2 for PE-PEO cross-linked copolymer compared to 0.17 mA/cm^2 for TiO_2-doped PS-*b*-PEO block copolymer).

To further demonstrate the application of these PE-PEO cross-linked SPEs at lower temperatures, galvanostatic cycling tests were also performed at 55 °C. The (^{70}PEOX$_{0.34}$)(^{34}PE$_{0.35}$)(^{5}PEG$_{0.31}$) polymer electrolyte exhibited C_d values of 564 C/cm^2 and 544 C/cm^2 at 0.40 mA/cm^2 and 0.65 mA/cm^2, respectively. These results are of significant interest because the high C_d values of these SPEs indicate their ability to inhibit dendrite growth, and the high ionic conductivity value of 7.0×10^{-4} S/cm at 55 °C supports their application for moderate temperature Li-metal battery operation. We are currently investigating the origins of the unique ability of our PE-PEO cross-linked SPEs to resist the proliferation of lithium dendrites in secondary batteries using metallic lithium anodes.

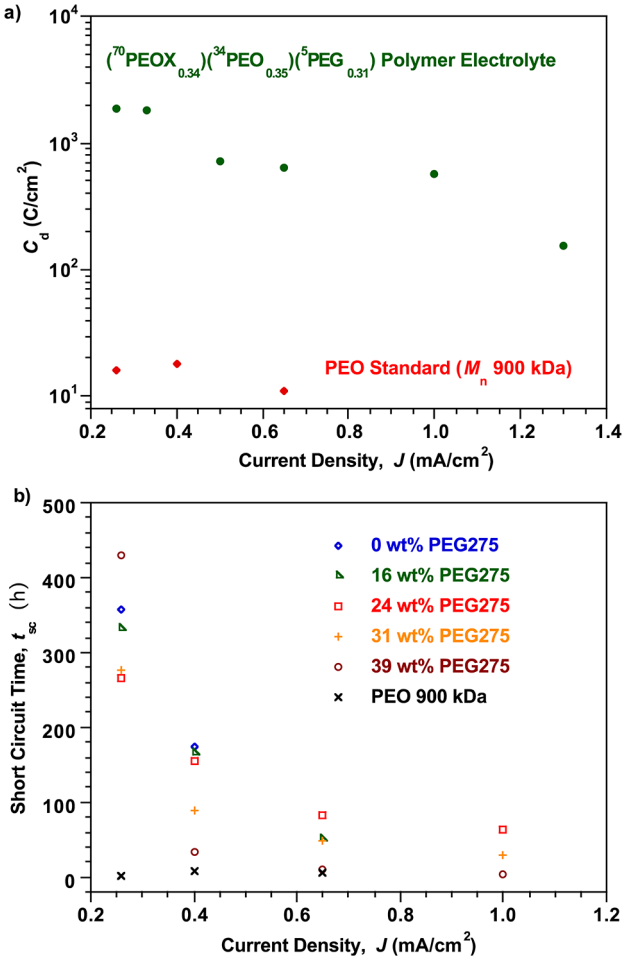

Figure 3. Dendrite tests. a) Galvanostatic cycling tests. The cycling data showing C_d as a function of current density at 90 °C for (^{70}PEOX$_{0.34}$)(^{34}PE$_{0.35}$)(^{5}PEG$_{0.31}$) polymer electrolyte (green ●) and PEO 900 kDa (red ♦). The cells were cycled at constant current density with each half cycle of 3 h until a short circuit was observed. See SI for more details. b) Galvanostatic polarization tests. Plot of short circuit time (t_{sc}) as a function of current density at 90 °C for various ^{70}PEOX electrolytes having different weight percent (wt %) of the plasticizer (PEG275). A PEO 900 kDa sample is also shown for comparison purposes.

Judging from the chemistry and shear mechanical properties of our PE-PEO cross-linked electrolytes, it is likely that Li^+ ions experience a tortuous nanoporous network of the conducting PEO phase as it migrates through the electrolyte. Such a network would facilitate migration of Li^+ ions, but could frustrate growth of micrometer-sized Li dendrites,[59,60] perhaps explaining the superior performance of our materials. Clearly a significant amount of research is needed to more concretely relate the unique structure of our materials to their ability to retard dendrite growth.

Dendrite resistance of selected SPEs was also examined using more conventional, but much harsher, galvanostatic polarization conditions. In this approach, the voltage response in a symmetric Li/SPE/Li cell is studied during continuous, one-direction plating at a prescribed current density. In these measurements, the Li/SPE/Li symmetric cells were polarized at current densities in the range 0.26–1.0 mA/cm^2 at 90 °C until the voltage drop was observed. Remarkably, we found that cells galvanostatically polarized at current densities of less than or

dx.doi.org/10.1021/ja502133j | J. Am. Chem. Soc. 2014, 136, 7395–7402

equal to 0.26 mA/cm^2 were able to plate the entire Li electrode without short circuit; in these cases, divergence of the potential halted testing. This finding means that a lithium battery operated under these conditions would not fail by dendrite-induced short circuits. To characterize the short circuit times (t_{sc}) at 0.26 mA/cm^2, it was necessary to laminate multiple Li foil layers (thickness ≈ 800 μm) to increase the amount of source Li in the electrode being stripped. Figure 3b shows the variation of the measured cell short circuit time, t_{sc}, with current density (0.26 mA/cm^2−1.0 mA/cm^2) for the cross-linked SPEs at 90 °C. Duplicate measurements were performed for two cross-linked samples at a specified current density value, and the results were found to be within 5% error. Since the tests were time-consuming, we performed only single measurements for rest of the cross-linked SPEs, and the results are shown in Figure 3b. The short circuit times of the SPEs (Table 2, entries 1−5) are significantly higher than those seen for the high molar-mass PEO-LiTFSI samples (M_n 900 kDa) made in our laboratory and all other reported SPEs to date.[18,61−63]

Rosso and co-workers reported that the onset of the dendrite growth and the growth velocity of the dendrites for PEO-LiTFSI electrolytes were in agreement with the prediction of the Chazalviel model.[18] However, while we find $t_{sc} \approx J^{-2}$, consistent with transport-limited dendrite growth assumed in the Chazalviel model, our experimental t_{sc} values are an order of magnitude or more higher than expected t_{sc} values based on this theory for most compositions (Figure S12 in the SI).[49] We conclude that there are additional physical features present in the PE-PEO cross-linked SPEs that provide higher than expected retardation of dendrites. Regardless of the dendrite growth inhibition mechanism, these PE-PEO cross-linked SPEs exhibit superior capacity to inhibit dendrite growth compared to all current materials over the entire range of current densities studied. In particular, at 0.26 mA/cm^2 and 90 °C, we observed t_{sc} values of 357 and 430 h for the unplasticized SPE (Table 2, entry 1) and 39 wt % plasticized SPE (entry 5) respectively. In terms of C_d, these values are equivalent to 334 C/cm^2 and 403 C/cm^2, although the test method is much more severe than galvanostatic cycling. By comparison, Rosso and co-workers reported a t_{sc} of 2 h at 0.25 mA/cm^2 and 90 °C for PEO-LiTFSI polymer electrolytes.[18] Liu and co-workers doped silica nanofillers[61] and ionic liquids[62] in the PEO-LiTFSI polymer electrolytes, and observed t_{sc} of 90 and 135 h, respectively, at 0.25 mA/cm^2 and 60 °C. They were able to increase the short circuit time to 168 h by doping it with both nano-SiO_2 and ionic liquid;[63] however, their reported short-circuit times (tests conducted at 60 °C) are still 2 times lower than our best PE-PEO cross-linked SPEs (tests conducted at 90 °C) reported herein. Note that all of the above referenced SPEs measure the short-circuit time using visualization cells with the interelectrode distance of 1 mm, instead of Li/polymer/Li symmetric coin cells used for our tests.[18,61−63] Due to much larger interelectrode separation distance, the dendrites will short these visualization cells slower than coin cells, suggesting that the reported short-circuit times in these reports are larger than expected in an actual cell. This suggests that the ability to resist the dendrite growth using the PE-PEO cross-linked SPEs disclosed herein is significantly higher than any other SPE reported in the literature to date.

CONCLUSIONS

In summary, we have developed a facile synthetic approach for the synthesis of a PE-PEO cross-linked SPE system that displays both high conductivity (>10^{-4} S/cm at 25 °C) and exceptional dendrite growth resistance. The cross-linked polymer electrolytes reported herein exhibit unprecedented levels of lithium dendrite growth resistance (demonstrated by highest C_d value and longest short circuit time reported to date, to the best of our knowledge). We believe that the combination of excellent dendrite growth resistance and high conductivity will allow the use of these SPEs in rechargeable LMP battery technologies for high energy density applications. In addition, these SPEs are also potential electrolyte components for next-generation high energy density Li battery technologies, lithium−sulfur and lithium−air batteries, which utilize Li metal as an anode material. We are currently studying the performance of these electrolytes in battery devices, and are initiating studies to determine morphology−property relationships. We anticipate that our polymer electrolyte design will spur investigation in the scientific community regarding the potential mechanisms of dendrite growth inhibition.

ASSOCIATED CONTENT

Supporting Information

Experimental procedures, characterization data, and spectra of all new compounds. Synthesis, thermal data, electrochemical characterization data, and rheology data of the solid polymer electrolytes. This material is available free of charge via the Internet at http://pubs.acs.org.

AUTHOR INFORMATION

Corresponding Authors

gc39@cornell.edu (G.W.C.)
laa25@cornell.edu (L.A.A.)

Funding

No competing financial interests have been declared.

Notes

The authors declare no competing financial interest.

ACKNOWLEDGMENTS

This material is based upon work supported as part of the Energy Materials Center at Cornell (EMC^2), an Energy Frontier Research Center funded by the U.S. Department of Energy, Office of Science, Office of Basic Energy Sciences under Award Number DE-SC0001086.

REFERENCES

(1) Tarascon, J. M.; Armand, M. *Nature* **2001**, *414*, 359−367.
(2) Goodenough, J. B.; Park, K. S. *J. Am. Chem. Soc.* **2013**, *135*, 1167−1176.
(3) Goodenough, J. B.; Kim, Y. *Chem. Mater.* **2010**, *22*, 587−603.
(4) Xu, K. *Chem. Rev.* **2004**, *104*, 4303−4417.
(5) Jacoby, M. *Chem. Eng. News* **2013**, *91* (6), 33−37.
(6) Vehicle Technologies Program, U. S. Department of Energy Multiyear program plan, 2011−2015. http://www1.eere.energy.gov/vehiclesandfuels/pdfs/program/vt_mypp_2011-2015.pdf. Accessed April 3, 2014.
(7) Armand, M.; Tarascon, J. M. *Nature* **2008**, *451*, 652−657.
(8) Scrosati, B.; Garche, J. *J. Power Sources* **2010**, *195*, 2419−2430.
(9) Zu, C. X.; Li, H. *Energy Environ. Sci.* **2011**, *4*, 2614−2624.
(10) Yoshimatsu, I.; Hirai, T.; Yamaki, J. *J. Electrochem. Soc.* **1988**, *135*, 2422−2427.
(11) Ishikawa, M.; Kawasaki, H.; Yoshimoto, N.; Morita, M. *J. Power Sources* **2005**, *146*, 199−203.
(12) Stark, J. K.; Ding, Y.; Kohl, P. A. *J. Electrochem. Soc.* **2011**, *158*, A1100−A1105.

(13) Zhamu, A.; Chen, G. R.; Liu, C. G.; Neff, D.; Fang, Q.; Yu, Z. N.; Xiong, W.; Wang, Y. B.; Wang, X. Q.; Jang, B. Z. *Energy Environ. Sci.* **2012**, *5*, 5701−5707.
(14) Gireaud, L.; Grugeon, S.; Laruelle, S.; Yrieix, B.; Tarascon, J. M. *Electrochem. Commun.* **2006**, *8*, 1639−1649.
(15) Mogi, R.; Inaba, M.; Jeong, S. K.; Iriyama, Y.; Abe, T.; Ogumi, Z. *J. Electrochem. Soc.* **2002**, *149*, A1578−A1583.
(16) Ota, H.; Wang, X. M.; Yasukawa, E. *J. Electrochem. Soc.* **2004**, *151*, A427−A436.
(17) Chazalviel, J.-N. *Phys. Rev. A* **1990**, *42*, 7355−7367.
(18) Rosso, M.; Gobron, T.; Brissot, C.; Chazalviel, J. N.; Lascaud, S. *J. Power Sources* **2001**, *97*−*8*, 804−806.
(19) Monroe, C.; Newman, J. *J. Electrochem. Soc.* **2005**, *152*, A396−A404.
(20) Stone, G. M.; Mullin, S. A.; Teran, A. A.; Hallinan, D. T., Jr.; Minor, A. M.; Hexemer, A.; Balsara, N. P. *J. Electrochem. Soc.* **2012**, *159*, A222−A227.
(21) Singh, M.; Odusanya, O.; Wilmes, G. M.; Eitouni, H. B.; Gomez, E. D.; Patel, A. J.; Chen, V. L.; Park, M. J.; Fragouli, P.; Iatrou, H.; Hadjichristidis, N.; Cookson, D.; Balsara, N. P. *Macromolecules* **2007**, *40*, 4578−4585.
(22) Fenton, D. E.; Parker, J. M.; Wright, P. V. *Polymer* **1973**, *14*, 589.
(23) Armand, M. B.; Chabagno, J. M.; Duclot, N. J. *Fast Ion Transport in Solids: Electrodes, and Electrolytes: Proceedings of the International Conference on Fast Ion Transport in Solids, Electrodes, and Electrolytes*; Lake Geneva, Wisconsin, U.S.A., May 21−25, 1979; Vashishta, P.; Mundy, J. N.; Shenoy, G. K., Eds; North Holland: New York, 1979.
(24) Le Nest, J. F.; Callens, S.; Gandini, A.; Armand, M. *Electrochim. Acta* **1992**, *37*, 1585−1588.
(25) Armand, M. *Solid State Ionics* **1983**, *9*−*10*, 745−754.
(26) Kono, M.; Hayashi, E.; Watanabe, M. *J. Electrochem. Soc.* **1998**, *145*, 1521−1527.
(27) Watanabe, M.; Nishimoto, A. *Solid State Ionics* **1995**, *79*, 306−312.
(28) Alloin, F.; Sanchez, J. Y.; Armand, M. *J. Electrochem. Soc.* **1994**, *141*, 1915−1920.
(29) Aihara, Y.; Kuratomi, J.; Bando, T.; Iguchi, T.; Yoshida, H.; Ono, T.; Kuwana, K. *J. Power Sources* **2003**, *114*, 96−104.
(30) Nishimoto, A.; Agehara, K.; Furuya, N.; Watanabe, T.; Watanabe, M. *Macromolecules* **1999**, *32*, 1541−1548.
(31) Snyder, J. F.; Carter, R. H.; Wetzel, E. D. *Chem. Mater.* **2007**, *19*, 3793−3801.
(32) Sun, X. G.; Reeder, C. L.; Kerr, J. B. *Macromolecules* **2004**, *37*, 2219−2227.
(33) Laik, B.; Legrand, L.; Chausse, A.; Messina, R. *Electrochim. Acta* **1998**, *44*, 773−780.
(34) Kim, G. T.; Appetecchi, G. B.; Carewska, M.; Joost, M.; Balducci, A.; Winter, M.; Passerini, S. *J. Power Sources* **2010**, *195*, 6130−6137.
(35) Rupp, B.; Schmuck, M.; Balducci, A.; Winter, M.; Kern, W. *Eur. Polym. J.* **2008**, *44*, 2986−2990.
(36) Matsumoto, K.; Endo, T. *J. Polym. Sci., Part A: Polym. Chem.* **2011**, *49*, 3582−3587.
(37) Schulze, M. W.; McIntosh, L. D.; Hillmyer, M. A.; Lodge, T. P. *Nano Lett.* **2014**, *14*, 122−126.
(38) Lee, J. I.; Kim, D. W.; Lee, C.; Kang, Y. *J. Power Sources* **2010**, *195*, 6138−6142.
(39) Wang, L.; Li, N.; He, X. M.; Wan, C.; Jiang, C. *Electrochim. Acta* **2012**, *68*, 214−219.
(40) Borghini, M. C.; Mastragostino, M.; Zanelli, A. *Electrochim. Acta* **1996**, *41*, 2369−2373.
(41) Morita, M.; Fukumasa, T.; Motoda, M.; Tsutsumi, H.; Matsuda, Y. *J. Electrochem. Soc.* **1990**, *137*, 3401−3404.
(42) Tatsuma, T.; Taguchi, M.; Oyama, N. *Electrochim. Acta* **2001**, *46*, 1201−1205.
(43) Tatsuma, T.; Taguchi, M.; Iwaku, M.; Sotomura, T.; Oyama, N. *J. Electroanal. Chem.* **1999**, *472*, 142−146.
(44) Robertson, N. J.; Kostalik, H. A.; Clark, T. J.; Mutolo, P. F.; Abruña, H. D.; Coates, G. W. *J. Am. Chem. Soc.* **2010**, *132*, 3400−3404.
(45) Shindoh, N.; Takemoto, Y.; Takasu, K. *Chem.—Eur. J.* **2009**, *15*, 12168−12179.
(46) The non-symmetrical design results in higher purity than the symmetrical coupling COE-O$(CH_2CH_2O)_n^-$ anions with *p*-dibromoxylene (see SI for details). For a related structure that was used to create polymer capsules *via* ROMP, see Emrick, T. S.; Brietenkamp, K. U.S. Patent 7,598,313, 2009.
(47) The reaction mixture for polymer film casting also contained hydrogenation catalyst (Crabtree's catalyst) and lithium bis(trifluorosulfonyl)imide (LiTFSI) ([EO]:[Li] = 18:1). The activity of the Grubbs G2 catalyst in the presence of TFSI anion and Crabtree's catalyst was confirmed by control experiments. COE (**2**) was copolymerized with PEG-grafted COE using Grubbs' G2 catalyst in the presence and absence of addtives to obtain copolymers, and the number average molecular weights (M_ns) of these polymers were determined using GPC. The activity of the Grubbs G2 catalyst was found to be comparable with or without the presence of additives. See SI for details.
(48) The efficiency of the hydrogenation step of the cross-linked unsaturated SPE films was confirmed by a control experiment. COE (**1**) was copolymerized with mono-COE-terminated PEG in the presence of lithium bis(trifluorosulfonyl)imide (LiTFSI) ([EO]:[Li] = 18:1) using Grubbs' G2 catalyst to obtain a non-crosslinked, unsaturated film. The film was subsequently hydrogenated in the same manner as for the cross-linked films. The hydrogenation reaction occured with 95% reduction of main-chain alkenes, as confirmed by ^{1}H NMR spectroscopy. See SI for details. Similar solid-state hydrogenation reactions have been previously reported using Crabtree's catalyst for polystyrene-*b*-polybutadiene-*b*-polystyrene block copolymer. For details, see:. Gilliom, L. R.; Honnell, K. G. *Macromolecules* **1992**, *25*, 6066−6088.
(49) See SI for details.
(50) He and co-workers observed similar cold crystallization peaks for PEO-$LiClO_4$ network polymer electrolytes in the presence of star plasticizers. See reference 39 for more details.
(51) Arora, P.; Zhang, Z. M. *Chem. Rev.* **2004**, *104*, 4419−4462.
(52) Berthier, C.; Gorecki, W.; Minier, M.; Armand, M. B.; Chabagno, J. M.; Rigaud, P. *Solid State Ionics* **1983**, *11*, 91−95.
(53) Barteau, K. P.; Wolffs, M.; Lynd, N. A.; Fredrickson, G. H.; Kramer, E. J.; Hawker, C. J. *Macromolecules* **2013**, *46*, 8988−8994.
(54) For the plasticized sample set, a new sample of PEOX cross-linker was synthesized to obtain approximately 76 EO units. Since it is challenging to control the exact amount of EO, the PEOX cross-linker with 70 EO units (^{70}PEOX) was employed instead of ^{76}PEOX cross-linker.
(55) Lee, Y. M.; Ko, D. H.; Lee, J. Y.; Park, J. K. *Electrochim. Acta* **2006**, *52*, 1582−1587.
(56) Cycling tests for ($^{70}PEOX_{0.34}$)($^{34}PE_{0.35}$)($^{5}PEG_{0.31}$) polymer electrolyte were performed on two different symmetric coin cells at 0.26 mA/cm^2 and 90 °C; C_d values of 1707 C/cm^2 and 1881 C/cm^2 were recorded for these cells, and the average value is reported in the text.
(57) Gurevitch, I.; Buonsanti, R.; Teran, A. A.; Gludovatz, B.; Ritchie, R. O.; Cabana, J.; Balsara, N. P. *J. Electrochem. Soc.* **2013**, *160*, A1611−A1617.
(58) The charge−discharge cycle used in the latest report was different from their previous studies on PS-*b*-PEO block copolymers (4 h compared to 3 h in the previous report).
(59) Tu, Z.; Kambe, Y.; Lu, Y.; Archer, L. A. *Adv. Energy Mater.* **2014**, *4*, 1300654/1−1300654/6.
(60) Tikekar, M. D.; Archer, L. A.; Koch, D. L. *J. Electrochem. Soc.* **2014**, *161*, A1−A9.
(61) Liu, S.; Imanishi, N.; Zhang, T.; Hirano, A.; Takeda, Y.; Yamamoto, O.; Yang, J. *J. Power Sources* **2010**, *195*, 6847−6853.
(62) Liu, S.; Imanishi, N.; Zhang, T.; Hirano, A.; Takeda, Y.; Yamamoto, O.; Yang, J. *J. Electrochem. Soc.* **2010**, *157*, A1092−A1098.

(63) Liu, S.; Wang, H.; Imanishi, N.; Zhang, T.; Hirano, A.; Takeda, Y.; Yamamoto, O.; Yang, J. *J. Power Sources* **2011**, *196*, 7681−7686.